Oncology and Translational Medicine
DOI 10.1007/s10330-014-0035-y
October 2015, Vol. 1, No. 5, P212–217

ORIGINAL ARTICLE

Improving patient care and accuracy of given doses in radiation therapy using in vivo dosimetry verification*

Ahmed Shawky Shawata[1] (✉), Tarek El Nimr[2], Khaled M. Elshahat[3]

[1] Radiation Oncology Center, Tanta Military Hospital, Egypt
[2] Department of Physics, Faculty of Science, Tanta University, Egypt
[3] Department of Clinical Oncology, Faculty of Medicine, Al Azhar University, Egypt

Abstract

Objective This work aims to verify and improve the dose given for cancer patients in radiation therapy by using diodes to enhance patient *in vivo* dosimetry on a routine basis. Some characteristics of two available semi-conductor diode dosimetry systems were evaluated.

Methods The diodes had been calibrated to read the dose at D_{max} below the surface. Correction factors of clinical relevance were quantified to convert the diode readings into patient dose. The diode was irradiated at various gantry angles (increments of 45°), various Field Sizes and various Source to Surface Distances (SSDs).

Results The maximal response variation in the angular response with respect to an arbitrary angle of 0° was 1.9%, and the minimum variation was 0.5%. The response of the diode with respect to various field sizes showed the minimum and the maximum variations in the measured dose from the diode; the calculated doses were –1.6% (for 5 cm × 5 cm field size) and 6.6% (for 40 cm × 40 cm field size). The diode exhibited a significant perturbation in the response, which decreased with increasing SSD. No discrepancies larger than 5% were detected between the expected dose and the measured dose.

Conclusion The results indicate that the diodes exhibit excellent linearity, dose reproducibility and minimal anisotropy; that they can be used with confidence for patient dose verification. Furthermore, diodes render real time verification of the dose delivered to patients.

Received: 7 December 2014
Revised: 27 March 2015
Accepted: 25 May 2015

Key words: *in vivo* dosimetry; diode dosimetry; external beam radiation therapy; uncertainty; water slab phantom; diode correction factors.

There are many potential error sources in radiation therapy treatment that can increase the uncertainty in the dose delivered to a patient to an unacceptable level. These error sources can be subdivided into four categories: (1) errors in the data transfer from the treatment-planning system (TPS) to the treatment equipment, (2) errors in the functioning of the treatment equipment, and errors that are patient related due to (3) setup errors or organ motion or (4) inaccuracies during the treatment-planning process.

Various methods may be chosen to detect and correct these errors. *In vivo* dosimetry with external beam radiation therapy in clinical practice can greatly improve tumor control and normal tissue sparing. On the other hand, this option makes the process of radiotherapy treatment more complex. There are many potential error sources in radiotherapy treatment that can increase the uncertainty in the dose delivered to a patient to an unacceptable level. Systematic errors in dose delivery for an individual patient can arise from incorrect linac calibration, machine output, radiation field flatness, the use of beam-modification devices, incorrect TPS calculations, and/or incorrect patient setup and internal organ motion. Therefore, several international organizations recommend performing *in vivo* dose measurements. Currently, the *in vivo* dosimetry method utilizes two diodes respectively positioned at the entrance and exit points along the central beam axis on the patient's skin surface. Thus, the patient isocenter

✉ Correspondence to: Ahmed Shawky Shawata. Email: physicist.ahmed@yahoo.com
* Supported by grants from Tanta University and Al-Hosain Hospital, Faculty of Medicine, Al Azhar University, Egypt.

dose (D_{max}) along the beam axis can be determined by a simple relationship and by reading the calibrated diodes.

However, this method requires periodic diode calibrations and accurate positioning of the detectors on the patient for every gantry angle, beam incidence angle, and beam energy. Moreover, this method has limitations when a patient presents asymmetric inhomogeneties along the beam central axis.

Clinical and experimental evidence has shown that even small dose changes can significantly reduce local tumor control. Furthermore, the International Commission on Radiological Units and Measurements (ICRU) recommends that the dose delivered to a tumor be within 5.0% of the prescribed dose [1]. Each of the many steps in treatment planning and execution contributes to the overall uncertainty in the dose delivered. Therefore, some organizations (ICRU [1–2], AAPM [3–4]) recommend that *in vivo* dosimetry (i.e., assessment of the dose directly in the patient) should be conducted. *In vivo* dosimetry treatment verification is very important; due to the presence of setup errors and internal organ motion, the planned dose may not be equal to the target dose. Each step can introduce errors that contribute to the final dose uncertainty, for example, geometry errors, errors introduced by transfer of treatment data from the treatment-planning system or simulator to the accelerator, errors in the beam setting, and so on [5].

Diodes are the most commonly used detector type for *in vivo* dosimetry. *In vivo* dosimetry is applied to assess the doses delivered to critical organs or to complex geometries in which dose prediction during treatment is difficult. *In vivo* dosimetry can also be used to monitor the doses delivered in special treatment techniques, and it is strongly recommended by numerous organizations such as ICRU and AAPM. Finally, the accuracy of the dose delivered can be checked directly only by means of *in vivo* dosimetry.

Materials and methods

Two linear accelerators and a Co^{60} unit were used with our *in vivo* dosimetry system. A Varian (Clinac 2300C/D) linac [6] was operated at photon energies of 6 and 15 MV and electron energies of 4, 6, 9, 12, 15, and 18 MeV. A Varian (Clinac 1800) linac [7] was operated at photon energies of 6 MV and 18 MV and electron energies of 6 Mev, 9 Mev, 12 Mev, 16 Mev, and 20 Mev. A cobalt-60 unit [8] is used with energy of 1.25 MV. The *in vivo* dosimetry system used with the diodes was IVD2 Model 1136 (Sun Nuclear Corporation, Model N-type, USA). The linacs were equipped for photons with two n-type Isorad photodiodes [Isorad (blue) 1–4 MV and Isorad (yellow) 6–12 MV] from Sun Nuclear Corporation (USA). Each photodiode was used for a single photon energy.

Bolus materials and a PTW plastic (solid water) phantom with a sided window of 30 cm × 30 cm × 30 cm size were used for this work. The dose at D_{max} on the central axis was determined by the use of a calibrated ion chamber. For convenience, the phantom was generally plastic. Usually the reference setup consisted of a gantry of 270°, source-to-surface distance (SSD) of 100 cm, field size of 10 cm × 10 cm, and dose of 1.00 cGy/MU at D_{max}. The linacs and Co^{60} unit were calibrated and checked daily for consistency by using a calibrated chamber to determine the actual dose at D_{max} that would yield a measurement of 1.00 cGy/MU. The diode was taped on the top of the phantom along the central beam axis. The internal buildup in the diode was expected to be sufficient to absorb electron contamination and to ensure electron equilibrium.

The treatment unit used for n-type Isorad (blue) semiconductor diode measurements was the Co^{60} unit (MSD Model Theratronics T780E) with 5-mm-thick polymethyl methacrylate serving as the buildup material. The X-ray beam from the Co^{60} unit had a nominal energy of 1.25 MV. Cobalt radiation reaches its maximum dose at 0.5 cm below the skin surface; therefore, it was especially well-suited for radiotherapy of the head, neck, and breast, and for tumors within 5 cm of the skin surface in other parts of the body.

The n-type Isorad (blue) semiconductor diode was used for all measurements in the range of 1–4 MV. This diode has a cylindrical geometry and a brass buildup cap with 1.4 g/cm^2 equivalent thickness. The detector and active diameters were 9.7 mm and 1.4 mm, respectively. The active detection area of this diode was 1.5 mm, with an active volume of 0.02 mm^3.

The treatment machines used for n-type Isorad (yellow) semiconductor diode measurements were dual-energy linear accelerators (Varian Clinac 2300 C/D, Varian Clinac 1800). The X-ray beams from these machines have nominal energies of 6 and 15 MV, respectively. All of the 3D conformal radiation therapy (3D-CRT) plans and measurements were conducted at 6 and 15 MV. The tissue phantom ratio at 20–10 cm depths in the linac was 0.67 for 6 MV and 0.74 for 15 MV, at a target-to-axis distance (TAD) of 100 cm. The n-type isorad (yellow) semiconductor diode was used for all measurements in the range of 6–12 MV. This diode has a cylindrical geometry and molybdenum buildup cap with 1.6 g/cm^2 equivalent thickness. The detector and active diameters were 9.7 mm and 1.4 mm, respectively. Its active detection area was 1.5 mm, with an active volume of 0.02 mm^3. All diode outputs were measured by an IVD2 Model 1136 system (Sun Nuclear Corporation, USA) consisting of two small electrometers interfaced with a PC.

A plastic phantom (water equivalent) was used for most diode tests and calibrations, with a 100 cm TAD at the center of the diode, a field size of 10 cm × 10 cm,

and 50 monitor units (MUs) of radiation delivered at the isocenter. The diode was used with 3D-CRT quality assurance for two patients on the Varian linear accelerator with 6 and 15 MV X-rays. The diode was placed in a plastic phantom at a 5 cm depth and with a TAD of 100 cm.

The diode was irradiated by the dose from the patient treatment plan, with the gantry and couch fixed at 0°. The reading obtained from the diode was compared with the doses planned by the Eclipse TPS and measured by an ionization chamber.

Calibration of the diode detectors was investigated by the diode correction factor (DCF) used in this paper for photons, which is the ratio of the dose at the diode to the diode reading. Using this ratio, the diode was calibrated to read the dose at D_{max} below the surface. SunPoint Diode-based instruments do not require warm-up or the application of a bias voltage prior to use, but ion chamber arrays can require up to 60 min and 10 Gy prior to use.

The diode response with respect to gantry angle was investigated by measuring the response to irradiation at various gantry angles, in increments of 45°. For all the irradiations, the diode was placed on the top edge of the treatment couch, with a field size of 10 cm × 10 cm, TAD of 100 cm, depth of 5 cm in the solid-water-slab phantom, and dose of 100 MUs. The angular response was recorded for nine angles around the diode and normalized to the response obtained for a gantry angle of 0°.

The diode response with respect to field size was investigated by measuring the response to irradiation with field sizes of 5 cm × 5 cm, 10 cm × 10 cm, 15 cm × 15 cm, 20 cm × 20 cm, 25 cm × 25 cm, 30 cm × 30 cm, 35 cm × 35 cm, and 40 cm × 40 cm, with a dose of 100 MUs and TAD of 100 cm. The diode calibration was conducted for a 10 × 10 cm^2 field size and TAD of 100 cm. The diode was irradiated at a dose rate of 300 MU/min. The dose measured by the diode was compared with the calculated dose. All doses were normalized to the dose measured with a field size of 10 cm × 10 cm. Correction-factor data were recorded for open, 15° wedged, 30° wedged, 45° wedged, and 60° wedged fields on the same day and under the same setup, but with an SSD of 100 cm.

The diode response with respect to SSD was investigated by measuring the response when the diode was placed at the surface of a 30 cm × 30 cm × 30 cm solid water slab phantom (at a depth of 1.5 cm) and was irradiated at SSDs of 70, 80, 90, 100, 110, 120, 130, 140, and 150 cm. The measurements were carried out for a 6 MV photon beam, field size of 10 cm × 10 cm, and dose rate of 100 MU/min. Correction-factor data were recorded for open, 15° wedged, 30° wedged, 45° wedged, and 60° wedged fields on the same day. Usually these measurements could be completed in less than 10 min, and thus the drift of the diode system could be neglected. From the five readings obtained above, we could obtain the relationship between the readings for the wedged fields and those for an open field.

Results

The calibration for SunPoint Diode detector products is very stable. The calibration factor can be obtained by finding the ratio of the readings from the ion chamber and diode; this calculation is done automatically by the IVD2 Model 1136 system (Sun Nuclear Corporation, USA) software [9]. The calibration factor was verified on a regular basis, because radiation damage affects the diode sensitivity. For p-type diodes, re-calibration was necessary after about 1 cGy. Re-calibration must be performed much more frequently for n-type diodes than for p-type diodes due to their faster decrease in sensitivity. Besides the calibration factor, which was determined under reference conditions (an SSD of 100 cm, a field size of 10 cm × 10 cm, and a dose of 1.00 cGy/MU at D_{max}), correction factors must be applied for accurate dosimetry. They originate from the variations in diode sensitivity with the dose per pulse, photon energy spectrum, temperature, and direction. The responses for gantry angles of 0° and 360° were equal, as in both cases the diode was in the same position facing the incident beam. Fig. 1 showed the normalized diode response with respect to gantry angle; the response was normalized with respect to that obtained at a gantry angle of 0°.

The maximum and minimum variations found in the angular response with respect to an arbitrary angle of 0° were 1.9% and 0.5%, respectively. The dose measured by the diode was compared with the calculated dose, and all doses were normalized to the dose at a measured field size of 10 cm × 10 cm. The normalized diode response with respect to field size was shown in Fig. 2. For entrance-field *in vivo* dosimetry, the diode reading increased almost linearly with increasing field size, with no significant variation in response, but beyond a field size of 10 cm × 10 cm, the diode reading increased to its maximum variation for a 40 cm × 40 cm field size. The minimum and maximum variations between the measured dose from the diode and the calculated dose were –1.6% (for a 5 cm × 5 cm field size) and 6.6% (for a 40 cm × 40 cm field size), respectively. Before a diode may be used in clinical applications, it was necessary to compare its response with that of a reference detector. The DCF of the 6 MV IsoRad photo-diode as a function of field size for open and different standard wedged fields was shown in Fig. 3. The correction factor (CF) did not change much when the field size changed. For open fields with an SSD of 100 cm, the range for CFs was generally within 1%, specifically, from 0.994 to 1.04. The change was up to 8% when the field size changed from 5 cm × 5 cm to 30 cm × 30 cm for open fields.

It was found that the DCF did not always increase with

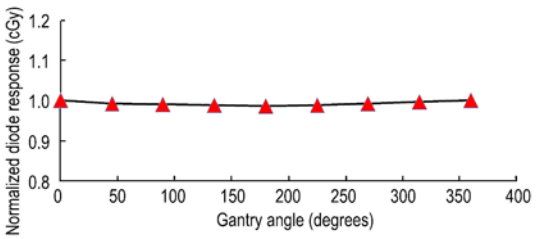

Fig. 1 Normalized response of diode with respect to gantry angle

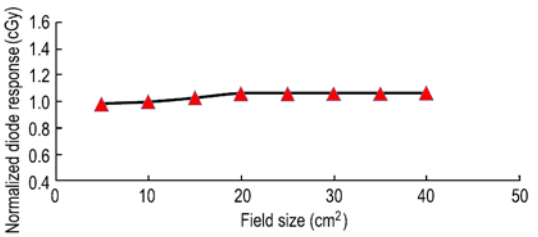

Fig. 2 Normalized response of diode with respect to field size

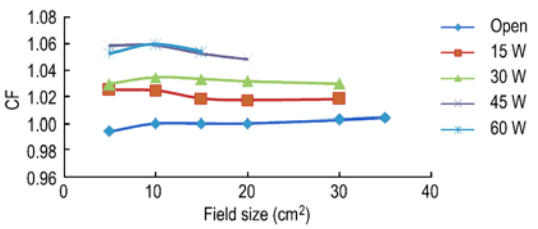

Fig. 3 Correction factor of 6 MV diode as a function of the field size for open field and different wedge angles, for entrance measurements with SSD 100 cm (max. field size for wedge 60˚ was 15 cm × 15 cm)

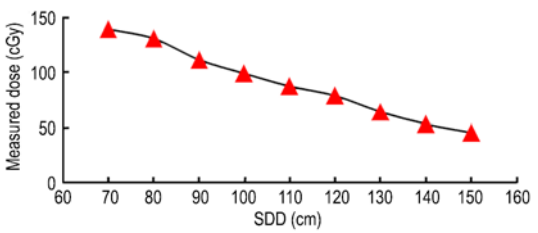

Fig. 4 Diode reading and the SSD dependence.

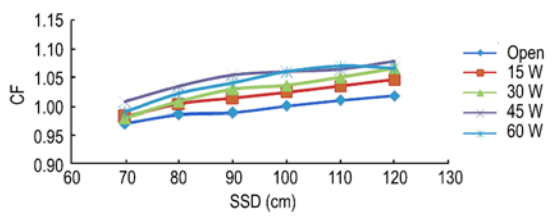

Fig. 5 DCFs as a function of the SSD for entrance measurements (6 MV photodiode with a field size of 10 cm x 10 cm)

increasing wedge angle. The field size dependences for open and 15˚ and 30˚ wedged fields were almost the same, but those for 45˚ and 60˚ wedged fields were larger, up to 6%. The diode response was recorded and compared with the calculated dose. Fig. 4 showed the response of the diode with respect to the SSD. The diode over-responded at SSDs of 70, 80, and 90 cm and exhibited significant perturbations in the response at these SSDs, which decreased with increasing SSD. For the SSD dependence of open 10 ×10 cm^2 fields, the range for CFs was from 0.97 to 1.018, in other words, within 4.8%, as shown in Fig. 5.

Discussion

It is well-known that angular dependence is theoretically not a factor in measurements carried out with this type of diode because of its cylindrical symmetry; however, to verify this assumption, the diode was irradiated at various gantry angles, in increments of 45°. Cylindrical detectors have a relatively small directional dependence when the incident beam rotates around the diode, with an effective sensitivity change of less than 2% for all angles. For isorad photodiodes, it is generally not necessary to consider the incident beam angle correction up to 60° because they are designed to have cylindrical symmetry [9]. The directional response is caused partly by the detector construction (including transmission through varying thicknesses of the buildup or cable at large angles) and partly by backscattering from the patient or phantom. The major directional dependence is determined by the angle between the beam axis and the axis of the cylindrical detector. Therefore, use of cylindrical diodes is required for oblique photon beams, such as breast tangents. In this study, the diode showed an almost isotropic response for various gantry angles. This characteristic has an advantage similar to that of using an ion chamber because the diode shape is cylindrical. The diode field size dependence indicates that the detector response increases with field size until it reaches a saturation behavior.

This behavior might be due to the presence of contaminating electrons and head-scattered low-energy photons. Because the variation was within 1%, it can be concluded that the DCF generally increases as the wedge angle increases. In other words, diodes under-respond when the wedge angle increases. The use of wedges causes a decrease in the intensity across the beam, changing the dose distribution from one point to another within the same field.

The necessary reading correction increases as the SSD increases, because diodes tend to underestimate the dose when the SSD increases beyond 100 cm. Scattered radiation from both overlying and underlying material might reach the sensitive part of the diode, contributing to the diode and ion chamber readings and potentially causing

Table 1 Comparison between *in vivo* dosimetry doses for head phantom for different detectors including thermoluminescence dosimeter, ionization chamber (IC), and diode system

Location	IC (cGy)	Detector 1 (cGy)	Detector 2 (cGy)	Mean (cGy)	% of Dose	TLD For 0.4Gy	Diode (cGy)	TPS (cGy)
Left lateral Field*	45.4	1505.965	1562.368	1534.167	85.23	42.96	45.20	46.0
Right lateral Field*	47.1	1524.651	1563.146	1543.899	85.77	43.23	43.31	47.0
Left Eye Lens	1.3	21.687	22.331	22.009	1.22	0.62	0.634	1.1
Right Eye Lens	1.3	23.884	24.409	24.1465	1.34	0.68	0.691	1.1

* TPS-based plan: planned for 6 MV beam: standard head phantom, parallel opposed lateral skull fields; open and 15 wedge beams for both right and left lateral fields. Dose of 180 cGy per fraction was delivered to normalization point in 28 fractions. All data were compared with data obtained from the treatment planning system (TPS)

overestimation or underestimation of the dose. Because the diode is placed at the surface and lacks an overlying layer, its reading is not very dependent on the phantom scatter but depends strongly on the head scatter. Therefore, the CF increases since the diode under-responds more with increasing in field size. The dependence of the CF on the SSD, for the same type of photodiode and with a 6 MV photon beam, was shown in Fig. 5. The CF for a wedged field is generally larger than that for the corresponding open field, because the dose per pulse becomes lower for a wedged field. When the SSD decreases, a number of contaminating electrons and scattered low-energy photons from the head are able to reach the sensitive part of the diode detector, so that the CFs of the ion chamber and of the diode reading decrease. As can be seen in Fig. 5, diodes still under-respond with increasing SSD for wedged fields. This behavior is primarily due to the change in dose per pulse caused by the SSD change. The diode reading is dependent on the phantom scatter factor and increases when the field size increases. We also expected that the field size correction factor for the diode would increase when the field size increased.

In vivo dosimetry tools can be used for verifying and improving the doses given to cancer patients in radiation therapy, and diodes can enhance patient *in vivo* dosimetry because they are suited for dosimetry both before and during treatment. Diodes are used for entrance or exit dose measurements to verify the entire planning process up to the delivery of treatment [10]. There were obvious errors associated with exit dose measurements, such as detector placement on the exit surface. The sources of measurement errors are also more difficult to identify when exit dose measurements are made. The entrance dose is far easier to predict. For these reasons, the entrance dose has been the favorite choice for institutions utilizing the IVD system [11].

In dosimetry using diodes, many factors can affect the response to radiation. For any diode detector, the sensitivity, reproducibility, correction factors due to the SSD, field size, wedge, radiation damage, and incident beam direction need to be considered. Additionally, diodes used with different linacs need to be characterized individually, because the spectra from different linacs may differ even at the same nominal energy. The diode sensitivity decreases with increasing cumulative dose. Scattered radiation from both overlying and underlying material might reach the sensitive part of the diode, contributing to the diode readings; the dose could be overestimated or underestimated as these complicating factors are dependent on the field size and/or SSD. Therefore, the commissioning or characterization of every diode individually is necessary for accurate dosimetry.

The results of *in vivo* entrance dose measurements were presented in Table 1. They show the mean percentage difference between the measured and expected doses, with a standard deviation of 2.6%. Comparison between this standard deviation and the estimated overall uncertainty of individual dose measurements (3%) indicates that the small discrepancies between the measured and mean values were due to limitations of the dosimetric system.

In this pilot study, no discrepancies larger than 5% between the expected dose and the measured dose were detected. Semiconductor detectors, that is to say, diodes, are the choice for treatment verification due to their high sensitivity, good spatial resolution, small size, ruggedness, absence of bias voltage, and independence from changes in air pressure. According to the diode response, the treatment plan or the setup of the entrance fields can be modified. This dosimetry method seems to be a useful tool for checking both the treatment plan and the appropriate setup of the patient in the treatment position. Diodes have a proven track record for providing *in vivo* doses with low intrinsic error.

Acknowledgments

All of the authors thank the anonymous reviewers for their helpful comments on the original manuscript.

Conflicts of interest

The authors indicated no potential conflicts of interest.

References

1. Hanna CL, Slade S, Mason MD, *et al*. Accuracy of patient positioning during radiotherapy for bladder and brain tumours. Clin Oncol, 1999, 11: 93–98.
2. Beckham WA, Keall PJ, Siebers JV. A fluence-convolution method to calculate radiation therapy dose distributions that incorporate random set-up error. Phys Med BIOL, 2002, 47: 3465–3473.
3. Almond PR, Biggs PJ, Coursey BM, *et al*. AAPM's TG-51 protocol for clinical reference dosimetry of high-energy photon and electron beams. Med Phys, 1999, 26: 1847–1870.
4. Therriault-Proulx F, Briere TM, Mourtada F, *et al*. A phantom study of an *in vivo* dosimetry system using plastic scintillation detectors for real-time verification of ^{192}Ir HDR brachytherapy. Med Phys, 2011, 38: 2542–2551.
5. Yuan J, Zheng Y, Wessels B, *et al*. Experimental validation of monte based on a virtual source model for tomotherapy in a RANDO phantom. Technol Cancer Res Treat, 2015, 9: 1533034615605007.
6. Deng J, Jiang SB, Kapur A, *et al.* Photon beam characterization and modelling for Monte Carlo treatment planning. Phys Med Biol, 2000, 45: 411–427.
7. Jornet N, Carrasco P, Jurado D, *et al*. Comparison study of MOSFET detectors and diodes for entrance *in vivo* dosimetry in 18 MV x-ray beams. Med Phys, 2004, 31: 2534–2542.
8. Baba MH, Mohib-Ul-Haq M, Khan AA. Dosimetric consistency of Co-60 teletherapy unit – a ten years Study. Int J Health Sci (Qassim), 2013, 7: 15–21.
9. Colussi VC, Beddar AS, Kinsella TJ, *et al*. *In vivo* dosimetry using a single diode for megavoltage photon beam radiotherapy: implementation and response characterization. J Appl Clin Med Phys, 2001, 2: 210–218.
10. Koole M, Lewis DM, Buckley C, *et al.* Whole-Body biodistribution and radiation dosimetry of 18F-GE067: a radioligand for *in vivo* brain amyloid imaging. J Nucl Med, 2009, 5: 818–822.
11. Planskoy B, Tapper PD, Bedford AM, *et al*. Physical aspects of total-body irradiation at the Middlesex Hospital (UCL group of hospitals), London 1988-1993: II. *In vivo* planning and dosimetry. Phys Med Biol. 1996, 41: 2327–2343.

DOI 10.1007/s10330-014-0035-y
Cite this article as: Shawata AS, Nimr TE, Elshahat KM. Improving patient care and accuracy of given doses in radiation therapy using *in vivo* dosimetry verification. Oncol Transl Med, 2015, 1: 212–217.